

Structural and molecular basis for the substrate positioning mechanism of a new PL7 subfamily alginate lyase from the arctic

Received for publication, July 5, 2020, and in revised form, September 13, 2020. Published, Papers in Press, September 23, 2020, DOI 10.1074/jbc.RA120.015106

Fei Xu^{1,‡}, Xiu-Lan Chen^{1,2,‡}, Xiao-Hui Sun¹, Fang Dong¹, Chun-Yang Li^{2,3}, Ping-Yi Li¹, Haitao Ding⁴, Yin Chen^{3,5}, Yu-Zhong Zhang^{1,2,3}, and Peng Wang^{2,3,*}

From the ¹State Key Laboratory of Microbial Technology, and Marine Biotechnology Research Center, Shandong University, Qingdao, China, the ²Laboratory for Marine Biology and Biotechnology, Pilot National Laboratory for Marine Science and Technology, Qingdao, China, the ³College of Marine Life Sciences, and Frontiers Science Center for Deep Ocean Multispheres and Earth System, Ocean University of China, Qingdao, China, the ⁴SOA Key Laboratory for Polar Science, Polar Research Institute of China, Shanghai, China, and the ⁵School of Life Sciences, University of Warwick, Warwick, Coventry, United Kingdom

Edited by Joseph M. Jez

Alginate lyases play important roles in alginate degradation in the ocean. Although a large number of alginate lyases have been characterized, little is yet known about those in extremely cold polar environments, which may have unique mechanisms for environmental adaptation and for alginate degradation. Here, we report the characterization of a novel PL7 alginate lyase AlyC3 from *Psychromonas* sp. C-3 isolated from the Arctic brown alga *Laminaria*, including its phylogenetic classification, catalytic properties, and structure. We propose the establishment of a new PM-specific subfamily of PL7 (subfamily 6) represented by AlyC3 based on phylogenetic analysis and enzymatic properties. Structural and biochemical analyses showed that AlyC3 is a dimer, representing the first dimeric endo-alginate lyase structure. AlyC3 is activated by NaCl and adopts a novel salt-activated mechanism; that is, salinity adjusts the enzymatic activity by affecting its aggregation states. We further solved the structure of an inactive mutant H127A/Y244A in complex with a dimannuronate molecule and proposed the catalytic process of AlyC3 based on structural and biochemical analyses. We show that Arg⁸² and Tyr¹⁹⁰ at the two ends of the catalytic canyon help the positioning of the repeated units of the substrate and that His¹²⁷, Tyr²⁴⁴, Arg⁷⁸, and Gln¹²⁵ mediate the catalytic reaction. Our study uncovers, for the first time, the amino acid residues for alginate positioning in an alginate lyase and demonstrates that such residues involved in alginate positioning are conserved in other alginate lyases. This study provides a better understanding of the mechanisms of alginate degradation by alginate lyases.

Alginate is a linear polysaccharide present in great abundance in brown seaweeds, accounting for ~40% dry weight of brown algae (1). Brown seaweeds are the most productive algae in marine ecosystems. For example, kelp forests produce large amounts of biomass rapidly, forming the basis of coastal food webs and constituting an important carbon sink (2). Therefore, alginate is an important marine polysaccharide and carrier of the marine carbon cycle. In addition to brown algae, alginate

has also been found in some red algae (3) and some marine bacteria belonging to the genera *Azotobacter* (4) and *Pseudomonas* (5). Alginate composes of two monomeric units, β -D-mannuronate (M) and its C5 epimer α -L-guluronate. These two units arrange in three ways: polymannuronate (PM), polyguluronate (PG), and heteropolymeric random sequences. Alginate is widely used as viscosifier, stabilizer, and gelling agent because of its unique gel-forming property. Alginate oligomers with various degree of polymerization may have different biological activities, such as regulating physiological processes in plants (6) and stimulating production of the cytokines (7).

Alginate lyases are synthesized by marine algae, marine mollusks, fungi, bacteria, and viruses, which play important roles in the degradation and assimilation of alginate. They degrade alginate via β -elimination reaction, targeting the glycosidic 1,4-*O*-linkage between the monomers, and generate oligosaccharide or monosaccharide products containing 4-deoxy-L-erythrohex-4-enopyranosyluronic acid as the nonreducing terminal moiety. Alginate lyases have wide applications in the agricultural, food, and pharmaceutical industry (8). Alginate lyases are promising enzymes for the treatment of chronic lung infection by *Pseudomonas aeruginosa* (9). The synergistic action of endo- and exolytic alginate lyases have remarkable potential for the production of biofuels by deconstructing the alginate-rich algal cell walls into monosaccharides (10, 11). Therefore, research on the characteristics and molecular catalytic mechanisms of alginate lyases is important to understand the degradation and recycling of alginate in the ocean and to facilitate the development of their industrial applications.

Based on the substrate specificities, alginate lyases can be classified into PM-specific lyases (EC 4.2.2.3), PG-specific lyases (EC 4.2.2.11), and bifunctional lyases that can degrade both PM and PG (EC 4.2.2.-). According to the lytic mode, alginate lyases are classified into endolytic and exolytic alginate lyases. Endolytic alginate lyases cleave glycosidic bonds inside polymers and release unsaturated oligosaccharides, whereas exolytic ones remove monomers or dimers from the ends of polymers. According to amino acid sequence similarity, alginate lyases are classified into 10 polysaccharide lyase (PL) families (PL5, 6, 7, 14, 15, 17, 18, 32, 34, and 36) in the

This article contains supporting information.

[‡]These authors contributed equally to this work.

*For correspondence: Peng Wang, wangpeng3331@ouc.edu.cn.

This is an Open Access article under the CC BY license.

16380 J. Biol. Chem. (2020) 295(48) 16380–16392

© 2020 Xu et al. Published under exclusive license by The American Society for Biochemistry and Molecular Biology, Inc.

Carbohydrate-Active enZYmes (CAZy) database (8, 12). Among these, the alginate lyases from the PL7, PL15, and PL17 families are mostly isolated from marine organisms (13).

Among the alginate lyase genes, the genes of the PL7 family alginate lyases are the most abundant and widely distributed in nature. The PL7 family contains alginate lyases from bacteria, eukaryotes, and viruses. Both endolytic and exolytic alginate lyases are found in this family (14). PL7 alginate lyases have broad substrate specificities, including PG-specific (15), PM-specific (16), and bifunctional enzymes (17). The PL7 family is further divided into five subfamilies in the CAZy database (18). Although the majority of the sequences in this family are classified into corresponding subfamilies, some sequences are still unclassified because of the lack of knowledge about their enzymatic characteristics.

The Arctic Ocean has extreme conditions noticeably for its low temperature and year-round existing ice cover. Bacteria in the Arctic Ocean are adapted to the extreme environment in their ecology and physiology. Therefore, the alginate lyases secreted by alginate-degrading strains from the Arctic may have unique properties and unique adaptive mechanisms. Up to now, only one thermostable alginate lyase from a hot vent in the Arctic mid-ocean ridge has been investigated (19). Thus, more research on alginate lyases from the polar environment is required.

Here, we report a novel PL7 alginate lyase AlyC3 from the bacterium *Psychromonas* sp. C-3, which was isolated from the brown alga *Laminaria* collected from the Arctic Ocean (20). Basing on multiple sequence alignment, we propose that AlyC3 and several other unclassified putative alginate lyases form a new PM-specific subfamily of PL7 (subfamily 6). We report the characterization of AlyC3 and demonstrate that AlyC3 is a polar alginate lyase with characteristics compatible with the polar environment with low temperatures and high salinity. Moreover, we solved the structure of AlyC3, the first dimeric endolytic alginate lyase, and found that dimerization is an adaptive strategy of AlyC3 to the seawater salinity. We report the structure of an inactive mutant in complex with disaccharides and uncover the key residues involved in the positioning of the substrate and subsequent catalysis. The discovery of this novel PL7 alginate lyase AlyC3 broadens our understanding of the PL7 alginate lyases and alginate degradation by cold-adapted alginate lyases of polar origins.

Results and discussion

AlyC3 is a new subfamily enzyme in the PL7 family

Psychromonas sp. C-3 is a cold-adapted strain isolated from the Arctic brown alga, which can use alginate as the carbon source for growth (20). We sequenced the whole genome of *Psychromonas* sp. C-3 and found that gene *alyC3* in the genome is annotated as an alginate lyase gene. *alyC3* is 861 bp in length and encodes a putative alginate lyase (AlyC3) of 286 amino acid residues with a predicted 20-residue signal peptide. Blast search results against the NCBI nonredundant protein database show that the AlyC3 protein (unless otherwise stated, AlyC3 discussed hereafter is the mature enzyme of 267 residues without the predicted signal peptide) has the highest identity (76.83%)

to AlyVOA, a characterized PL7 alginate lyase from *Vibrio* sp. O₂ isolated from seawater in the Mihonoseki Harbor in Japan (21).

Although most of the PL7 enzymes in the CAZy database are classified into five subfamilies, some PL7 lyases have not yet been attributed to any subfamily because of their low sequence similarities to others in the database. We performed phylogenetic analysis of AlyC3 with 36 other PL7 alginate lyases from existing subfamilies and 14 unclassified sequences using maximum likelihood, neighbor joining, and minimum evolution methods (Fig. 1 and Figs. S1 and S2). These include representative alginate lyases from each subfamily, including six sequences from subfamily 2 and seven sequences from subfamily 4. It is worth noting that only one subfamily 4 alginate lyase is characterized, and no subfamily 2 alginate lyase is characterized to date. The result shows that these sequences are grouped into six clusters (Fig. 1 and Figs. S1 and S2). Enzymes that have been attributed to subfamilies in the CAZy database are assigned to the corresponding subfamily clusters. AlyC3 clustered with six other sequences, forming a separate monophyletic branch. We therefore propose that these seven enzymes form a new subfamily, subfamily 6, of the PL7 family. Among the enzymes of subfamily 6, four have been characterized previously, that is, AlyVOA (ABB36771.1) (21), AlyVOB (ABB36772.1) (21), AlxM (CAA49630.1) (22), and A9mT (BAH79131.1) (23). All these four alginate lyases prefer PM as the substrate.

AlyC3 is a cold-active and PM-specific endo-alginate lyase

To characterize AlyC3, gene *alyC3* was cloned from the genome of *Psychromonas* sp. C-3 and overexpressed in *Escherichia coli* without the putative signal peptide sequence. With alginate sodium as the substrate, the purified recombinant AlyC3 exhibited the highest activity at pH 8.0 and 20 °C and retained 48.2% of its maximum activity at 1 °C (Fig. 2, A and B). AlyC3 showed poor thermal stability, unstable at temperatures of 30 °C and above (Fig. 2C). These characteristics indicate that AlyC3 is a cold-active enzyme, well-adapted to the cold and alkaline environment of the Arctic Ocean. AlyC3 is the first reported cold-active alginate lyase isolated from the polar region. The only Arctic origin alginate lyase reported so far is AMOR_PL7A from an Arctic hot vent, which is a thermophilic enzyme, with the highest activity at 65 °C and pH 6.0 (19).

AlyC3 displayed the highest activity toward PM and no activity toward PG (Fig. 2D), indicating that AlyC3 is a PM-specific lyase. As shown in Fig. 1, PL7 lyases from different subfamilies have different substrate specificity characteristics. All of the four characterized subfamily 1 alginate lyases are bifunctional, whereas most alginate lyases from subfamilies 3 and 5 are PG-specific or bifunctional. The only characterized subfamily 4 enzyme is a glucuronan lyase. AlyC3 and the other four characterized alginate lyases of subfamily 6, including AlyVOA, AlyVOB, AlxM, and A9mT, are all PM-specific alginate lyases (21–23).

AlyC3 could not degrade trimannuronate into smaller products but could degrade tetramannuronate into ΔMM (Δ represents 4-deoxy-L-erythro-hex-4-enopyranosyluronic acid) and

Substrate positioning of an alginate lyase

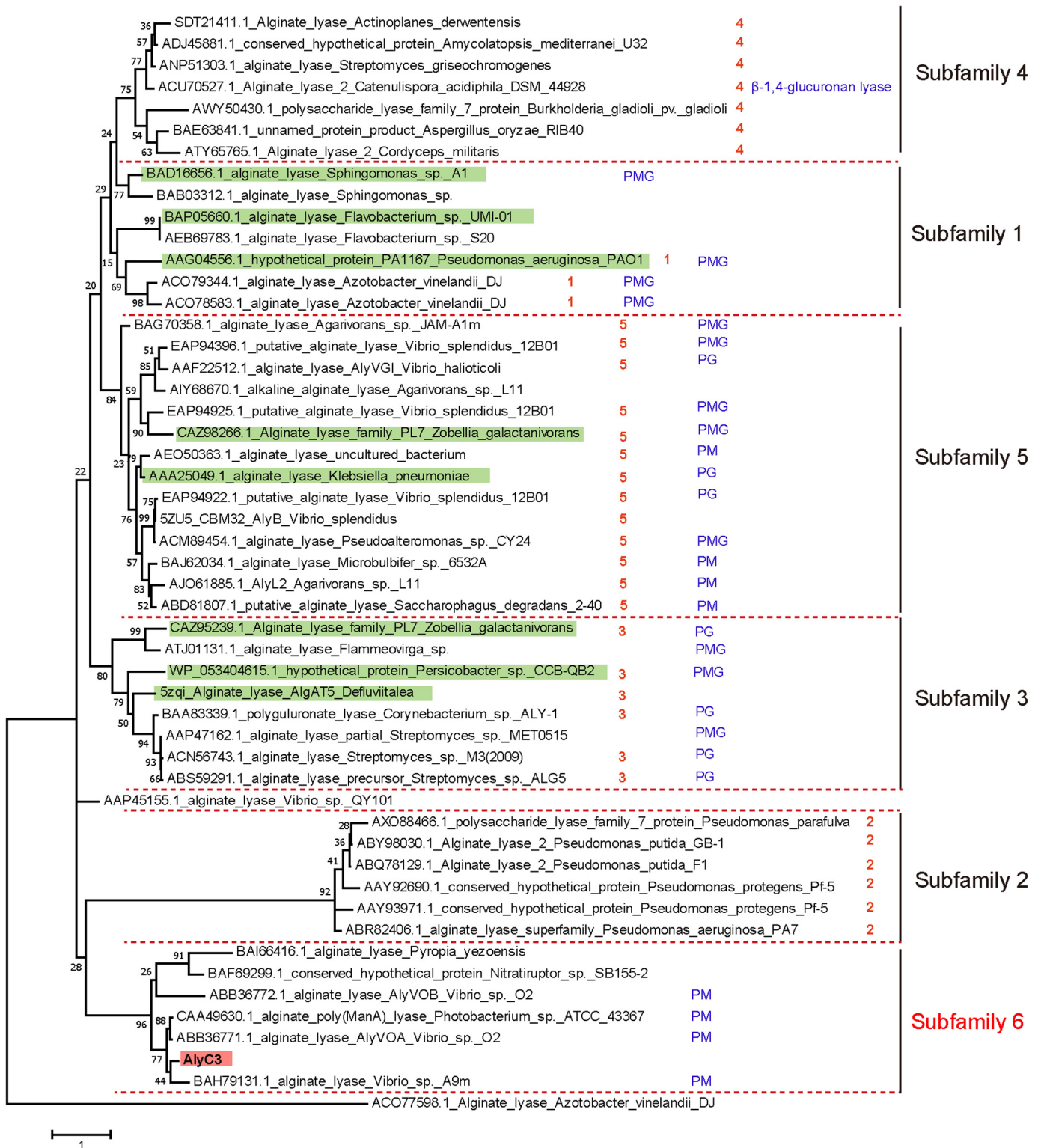


Figure 1. Phylogenetic analysis of AlyC3 and other PL7 lyases from different subfamilies. The unrooted phylogenetic tree was constructed by using the maximum likelihood with a Jones–Taylor–Thornton matrix–based model using the catalytic domains. Bootstrap analysis of 1000 replicates was conducted. Clusters of proteins are separated by dotted lines. The subfamily and the substrate specificity were marked in red numbers and blue annotations according to the CAZy database. Enzymes highlighted in green are structure-solved. AlyC3 is highlighted in red.

monosaccharide, suggesting that the minimum substrate for AlyC3 is tetramannuronate. When using pentamannuronate as the substrate, ΔMMM, ΔMM, and a trace amount of ΔM and Δ

were produced. When hexmannuronate was degraded by AlyC3 for 10 min, a large amount of ΔMM and small amounts of ΔMMMM, ΔMMM, and ΔM were produced. These results

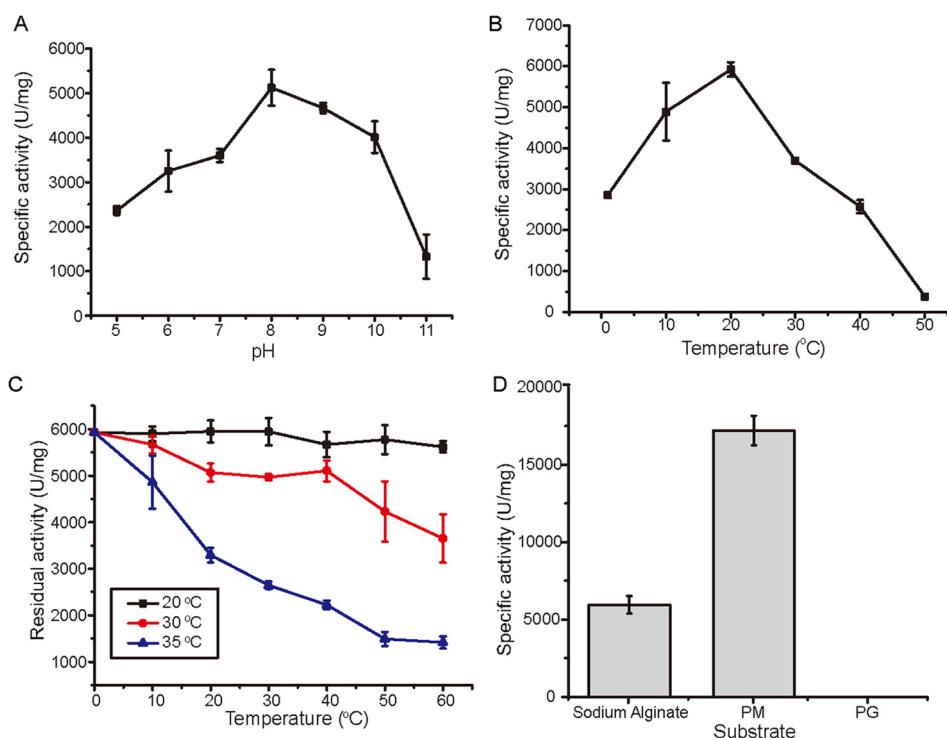


Figure 2. Enzymatic characterization of AlyC3. *A*, the effect of pH on the activity of AlyC3 toward sodium alginate. Experiments were conducted at 20 °C for 5 min in a 200- μ l mixture containing 0.6 μ g/ml enzyme and 2 mg/ml sodium alginate in 50 mM Britton–Robinson buffer ranging from pH 5 to 11. *B*, the effect of temperature on the activity of AlyC3 toward sodium alginate. A 200- μ l reaction mixture containing 0.6 μ g/ml enzyme and 2 mg/ml sodium alginate in 50 mM Tris-HCl (pH 8.0) was incubated at 20 °C for 5 min. *C*, the effect of temperature on the stability of AlyC3. AlyC3 was incubated at different temperatures for 0 to 60 min, and the residual activities were measured at 20 °C and pH 8.0. *D*, the substrate specificities of AlyC3 toward sodium alginate, PM, and PG.

indicate that AlyC3 is an endolytic lyase, with Δ MM as the main product (Fig. 3).

Altogether, these results show that AlyC3 is a cold-active and PM-specific endo-alginate lyase. Several cold-active alginate lyases have been reported, which all have an optimum temperature no less than 30 °C (24–28). Therefore, AlyC3 has the lowest optimum temperature (20 °C) among reported alginate lyases to date.

AlyC3 is a dimeric endo-alginate lyase

Similarity search at the Protein Data Bank (PDB) database showed that no suitable structure model can be used for AlyC3 structure construction. Therefore, we solved the crystal structure of WT AlyC3 by single-wavelength anomalous dispersion method using a selenomethionine derivative. The crystal of WT AlyC3 belongs to the P 21 21 21 space group, and the structure was solved to 2.1 Å resolution (Table 1). Structure data show that each asymmetric unit contains two AlyC3 molecules of 264 residues (Asn²–Glu²⁶⁵), and each molecule binds one glycerol molecule and one succinic acid molecule, both of which came from the buffer solution (Fig. 4A).

The overall structure of the AlyC3 monomer is a β -jelly roll fold, which is common in alginate lyases and is adopted by alginate lyases from families PL7, 14, 18, and 36 (29–32). The structure of AlyC3 contains four helices and two large β -sheets (sheet A and sheet B). Sheet A (SA) consists of nine β -strands: SA1 (Glu⁴³–Phe⁴⁵), SA2 (Ser²⁸–Ile³²), SA3 (His⁷⁶–Val⁸³), SA4 (Leu²³⁶–Ala²⁴¹), SA5 (Val²⁴²–Gln²⁴⁶), SA6 (Asn¹¹⁹–Gly¹³⁰), SA7 (Leu¹⁴³–Lys¹⁴⁹), SA8 (Gly¹⁵⁷–Lys¹⁶⁴), and SA9 (Tyr¹⁹⁰–

Gly¹⁹⁶). Sheet B (SB) consists of seven β -strands: SB1 (Phe⁵⁹–Asp⁶²), SB2 (Asp⁶⁶–Lys⁷³), SB3 (Met²⁵¹–Leu²⁶⁴), SB4 (Leu⁹⁵–Ile¹⁰⁴), SB5 (Thr²⁰⁴–Gly²¹¹), SB6 (Gln²¹⁴–Val²¹⁹), and SB7 (Lys²²²–Asp²²⁸) (Fig. 4B). All of the β -strands use an antiparallel arrangement. The sheet A shapes a cleft and forms a positively charged groove in the middle of AlyC3. The succinic acid and glycerol molecules are mainly bound to the SA7 and SA4, respectively (Fig. 4B).

Gel filtration data showed that AlyC3 exists as a dimer in 0.5 M NaCl solution, consistent with the structure result (Fig. 4C). In AlyC3 dimer, the two subunits are arranged upside down in parallel (Fig. 4A). Almost all the residues involved in the interfacing of the two monomers are on the loops connecting SA3–SB4, SA6–SA7, SA8–SA9, and SB7–SA4 of each monomer (Fig. 4, A and B). Up to now, no endolytic dimeric alginate lyases have been reported, and only the structures of two dimeric exolytic alginate lyases (AlyGC from PL6 and AlyA5 from PL7) have been reported (14, 33). Thus, AlyC3 represents the first dimeric structure of endolytic alginate lyases. The interfaces of the two dimeric exolytic alginate lyases are different from that of AlyC3 (Fig. 4D). The interface of AlyA5 dimer mainly occurs on the loop connecting SA3 and SB4 of each monomer, and its interface area is apparently smaller than that of AlyC3. Different from the single-domain AlyC3 and AlyA5, AlyGC is a two-domain enzyme, consisting of a C-terminal domain and an N-terminal domain, and most of the interface of AlyGC between the two monomers occurs between the C-terminal domains.

Although AlyC3 shows low sequence identity and different aggregation state from the other structure-solved PL7 alginate

Substrate positioning of an alginate lyase

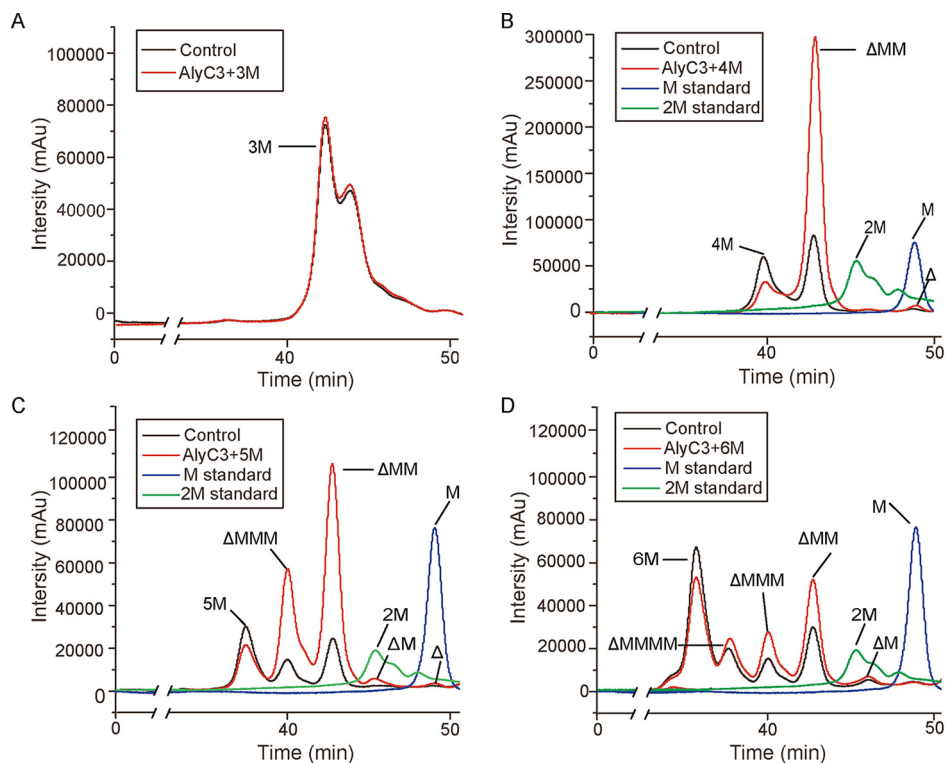


Figure 3. Degradation products of AlyC3 toward different mannuronate oligosaccharides. Tri- to hexaoligosaccharides were used as the substrates, corresponding to A–D, respectively. The reaction was carried out at 20 °C for 10 min in a 200- μ l mixture containing 0.7 μ g/ml AlyC3 and 2 mg/ml substrate in 50 mM Tris-HCl (pH 8.0) containing 0.5 M NaCl. The resultant degradation products were analyzed by HPLC on a Superdex Peptide 10/300 GL column at a flow rate of 0.35 ml/min using 0.2 M ammonium hydrogen carbonate as the running buffer. Control group was performed with pre-heat-inactivated AlyC3. M, 2M, 3M, 4M, 5M, and 6M represent mannuronate monomer, dimer, trimer, tetramer, pentamer, and hexamer, respectively.

lyases, the topological structure of AlyC3 monomer is similar to those of the other PL7 alginate lyases. It is most similar to that of the alginate lyase A1- $\text{I}\ddot{\text{I}}$ with a root-mean-square deviation (RMSD) of 2.0 Å and a Z score of 23.4 (34). Despite their similar topological structures, AlyC3 has two notable differences compared with all the other 10 structures of PL7 alginate lyases. The first difference is on loop 1 (Fig. 4E). The 10 reported PL7 structures all adopt a long and flexible loop 1. Yamasaki and coworkers (35) proposed that loop 1 opening is necessary for substrate binding when the catalytic reaction is initiated. However, the loop 1 of AlyC3 is quite short, composing only two residues (Asn⁷⁴ and Asp⁷⁵), too short to form an open state or a closed state. Thus, the initiation stage of AlyC3 is perhaps different from those of the other studied PL7 alginate lyases. The second difference is on loop 2 (Fig. 4E). Loop 2 is located at one end of the active center. Loop 2 of AlyC3 (residues 165–189) is cross-linked by a disulfide bond formed between Cys¹⁷⁰ and Cys¹⁸⁴, which is not observed in other studied PL7 alginate lyase structures. In addition, as mentioned above, many interfacing residues are on loop 2. Hence, loop 2 is essential for maintaining both the configuration of the active center and the unique dimer structure of AlyC3.

Dimerization is an adaptive strategy of AlyC3 to the seawater salinity

Because AlyC3 originates from a bacterium isolated from the Arctic Ocean, we studied the effect of NaCl on the activity of

AlyC3. AlyC3 showed the highest activity at 0.5 M NaCl, 2.9 times of its activity at 0 M NaCl, which reflects the adaptation of AlyC3 to the Arctic Ocean where the average salt concentration is \sim 0.5 M (36). In addition, AlyC3 still retained high activity at NaCl concentrations more than 0.5 M. Its activity at 3 M NaCl was still higher than that at 0 M NaCl (Fig. 5A), which may indicate the adaptation of AlyC3 to fluctuation in salinity in the Arctic Ocean salinity with seasons. We further investigated the effect of NaCl on the aggregation state of AlyC3. As shown in Fig. 5 (B and C), AlyC3 is dimers in 0.5 M NaCl solution but tends to be polymers in solutions with NaCl concentration less than 0.5 M and to be monomers in solutions with NaCl concentration more than 0.5 M. Taken together, these results indicate that dimeric AlyC3 in 0.5 M NaCl has the highest activity. Thus, it can be speculated that dimerization is a strategy adopted by AlyC3 to adapt to the seawater salinity (\sim 0.5 M) of the Arctic Ocean. Moreover, the surface of dimeric AlyC3 is full of hydrophilic amino acids. The front of the catalytic cavity is more positively charged, and the back is more negatively charged (Fig. 5D). The strong surface charges may help AlyC3 to resist the hydrophobicity and the loss of hydration layer caused by high salinity (37).

Several salt-activated alginate lyases have been reported previously (27, 38). The salt activation of alginate lyase AlyPM resulted from the enhancement of its substrate affinity to NaCl (27). Another example is AlgM4, whose secondary structure can be altered by NaCl, probably resulting in the enhancement

Table 1
Diffraction data and refinement statistics of SeMet-AlyC3, WT AlyC3, and H127A/Y244A-M2

| Parameters | SeMet AlyC3 | WT AlyC3 | H127A/Y244A-M2 |
|------------------------------------|---------------|---------------|----------------|
| Data collection | | | |
| Space group | P 4 | P 21 21 21 | C 1 2 1 |
| Unit cell ^a | | | |
| <i>a</i> (Å) | 44.38 | 44.90 | 80.87 |
| <i>b</i> (Å) | 44.38 | 45.60 | 106.41 |
| <i>c</i> (Å) | 306.68 | 305.88 | 79.29 |
| α (°) | 90.00 | 90.00 | 90.00 |
| β (°) | 90.00 | 90.00 | 93.85 |
| γ (°) | 90.00 | 90.00 | 90.00 |
| Wavelength (Å) | 0.9791 | 0.9791 | 0.9791 |
| Resolution (Å) | 50.00–2.80 | 50.00–2.10 | 50.00–1.46 |
| | (2.80–2.90) | (2.10–2.18) | (1.46–1.51) |
| Redundancy | 7.5 (7.4) | 7.0 (6.6) | 3.4 (3.3) |
| Completeness (%) | 99.9 (100.0) | 98.8 (99.3) | 98.1 (99.5) |
| R_{merge}^b | 0.123 (0.438) | 0.110 (0.410) | 0.035 (0.219) |
| I/σ | 29.54 (7.52) | 31.84 (5.96) | 40.78 (4.71) |
| Refinement statistics | | | |
| Resolution (Å) | | 43.08–2.10 | 30.35–1.46 |
| | | (2.10–2.18) | (1.51–1.46) |
| R_{work} (%) | | 20.70 (25.69) | 15.90 (21.02) |
| R_{free} (%) | | 27.11 (30.10) | 17.20 (23.57) |
| B-factor (Å ²) | | | |
| Protein | | 35.28 | 23.29 |
| Solvent | | 38.23 | 38.29 |
| Ligands | | 38.35 | 51.07 |
| RMSD from ideal geometry | | | |
| Length (Å) | | 0.008 | 0.014 |
| Angles (°) | | 0.97 | 1.24 |
| Ramachandran plot (%) ^c | | | |
| Favored | | 95.00 | 97.00 |
| Allowed | | 4.20 | 3.00 |

^aNumbers in parentheses refer to data in the highest resolution shell.

^b $R_{\text{merge}} = \sum_{\text{hkl}} \sum_i |I(\text{hkl})_i - \langle I(\text{hkl}) \rangle| / \sum_{\text{hkl}} \sum_i \langle I(\text{hkl})_i \rangle$.

^cThe Ramachandran plot was calculated by the PROCHECK program in the CCP4i program package.

of its affinity to substrates and its ability to resist thermal denaturation (38). Different from the salt-activation mechanisms of AlyPM and AlgM4, our results indicate that the salt-activation mechanism of AlyC3 is to retain a dimeric quaternary structure.

Identification of important residues for catalysis in AlyC3

To obtain an inactive AlyC3 mutant for enzyme–substrate complex crystallization, site-directed mutations on AlyC3 were conducted based on structural analysis. The result indicated that when His¹²⁷ or Tyr²⁴⁴ was mutated to alanine, the mutated AlyC3 was almost inactive toward PM. Thus, the two single mutants H127A and Y244A and the double mutant H127A/Y244A were crystallized with alginate oligosaccharides, respectively. Finally, the crystal structure of H127A/Y244A in complex with dimannuronate (M2) (H127A/Y244A-M2) was solved to 1.5 Å resolution. In the complex structure, each H127A/Y244A molecule binds an M2 substrate and a malonate molecule from the buffer solution (Figs. 6, A and B). The M2 molecule is bound in the positively charged groove of AlyC3. The positive charge of the groove is beneficial for the binding of the negatively charged alginate chain. The structures of H127A/Y244A-M2 monomer and WT AlyC3 monomer are fairly similar, with an RMSD of 0.41 Å (Fig. 6C).

Alginate cleavage is a typical acid-base catalysis of the β -elimination reaction. The β -elimination reaction occurs

between the +1 site and –1 site of the alginate chain and the catalysis requires neutralization of the negative charge on the +1 site carboxylic group (39). Sequence alignment shows that His¹²⁷, Tyr²⁴⁴, Arg⁷⁸, and Gln¹²⁵ are strictly conserved in the PL7 alginate lyases (Fig. 6D). The corresponding residues of His¹²⁷, Tyr²⁴⁴, Arg⁷⁸, and Gln¹²⁵ in the PL7 lyases A1-II, FLA-lyA, and AlyA1PL7 are the key residues required for the β -elimination reaction against alginate (14, 16, 35). Thus, they are also likely the key residues involved in the catalytic process in AlyC3. Four possible binding subsites of mannuronate molecules are found in the structure of H127A/Y244A-M2 (one binding subsite is occupied by the malonate molecule) (Fig. 6, A and E), which is consistent with the biochemical result showing that tetramannuronate is the minimal substrate for AlyC3 (Fig. 3B). The bound M2 molecule has interactions with His¹²⁷, Tyr²⁴⁴, Arg⁷⁸, and Gln¹²⁵. Combining with the result that the cleavage of tetramannuronate produces trisaccharide and monosaccharide (Fig. 3B), we suggest that the M2 molecule binds at the subsites of –1 and +1 (Fig. 6A). His¹²⁷ and Tyr²⁴⁴ are the two residues that are close to the C5 of the +1 subsite and O4 of the –1 subsite of the M2 molecule. In addition, Arg⁷⁸ and Gln¹²⁵ are close to the carboxyl group of the +1 subsite mannuronate molecule. When His¹²⁷, Tyr²⁴⁴, or Gln¹²⁵ was mutated to alanine, the mutants lost the activity toward PM (Fig. 6F), and when Arg⁷⁸ was mutated to alanine, the activity of the mutant toward PM is greatly decreased (Fig. 6F). These results suggest that His¹²⁷ and Tyr²⁴⁴ are the catalytic base and the catalytic acid of the reaction, respectively, and Arg⁷⁸ and Gln¹²⁵ are necessary for the neutralization of the negative charge on the carboxylic group of +1 subsite.

Identification of important residues for substrate positioning in AlyC3

In H127A/Y244A-M2, Tyr⁴⁴, Arg⁸², Lys¹²⁹, His¹⁴¹, Lys¹⁷¹, Tyr¹⁹⁰, and Gln²⁴⁶ are the hydrophilic residues around the active cavity, most of which are basic amino acids that are positively charged at nearly neutral pH. Mutations on these residues decreased the activity of AlyC3 (Fig. 6F). Thus, these residues may be required for the binding of the substrate. Therefore, the kinetic parameters of the mutants were investigated (Table 2). Surprisingly, the K_m values of the mutants R82A and Y190A did not increase but remained unchanged or slightly decreased compared with that of the WT AlyC3, indicating that these mutations on the two residues had little effect on the affinity of the enzyme to the substrate. In contrast, the V_{max} values of these mutants reduced significantly compared with that of the WT AlyC3. These results imply that these mutations affect the catalytic efficiency of the reaction. However, these residues are located at the two ends of the catalytic cavity, both of which are far away from the active center (Fig. 6E). Alginate is a long-chain substrate with repeated monosaccharide units. Thus, during the reaction process, in addition to the substrate binding, correct positioning of repeated units is also important for initiating the catalysis. Positioning error may change the distances between the catalytic base/acid and the substrate, thereby affecting the catalytic efficiency of the reaction. Basing on the aforementioned results from site-directed

Substrate positioning of an alginate lyase

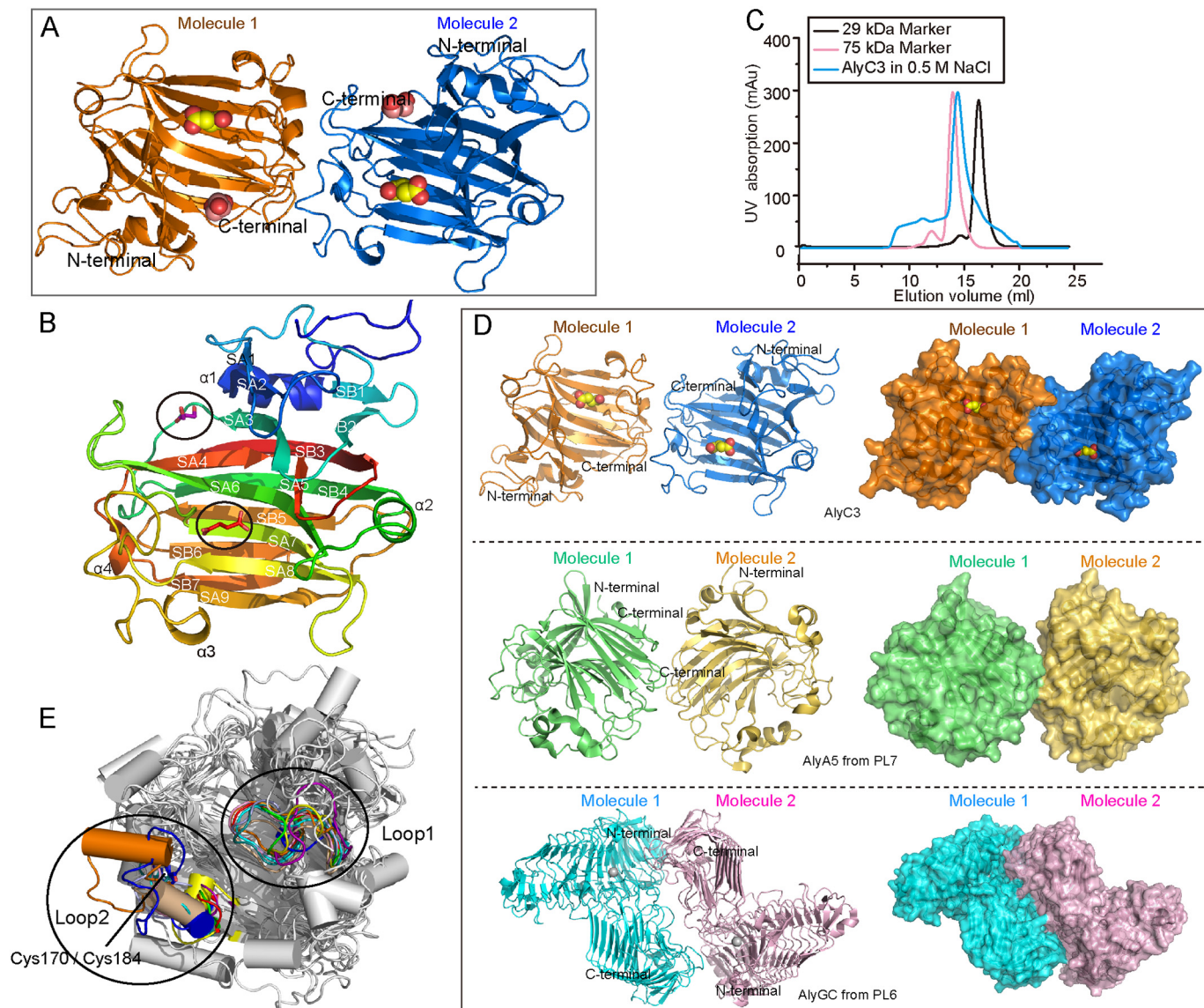


Figure 4. Analysis of the overall structure of AlyC3. *A*, the overall structure of the dimeric AlyC3. The bound succinic acid and glycerol molecules are shown as *yellow* and *pink spheres*, respectively. *B*, the overall structure of the monomeric AlyC3. The structure is depicted in *rainbow colors* from *blue* in the N-terminal region to *red* in the C-terminal region. The succinic acid and glycerol are shown as *red* and *purple sticks*, respectively. *C*, gel filtration analysis of the form of AlyC3 in solution using conalbumin (75 kDa) and carbonic anhydrase (29 kDa) as protein size standards. The molecular mass of dimeric AlyC3 is 6.1 kDa. *D*, the comparison of the interfaces of the dimeric AlyC3 with other dimeric alginate lyases. All three enzymes are shown as cartoon and surface views, respectively. *E*, comparison of loops 1 and 2 in PL7 structure-solved alginate lyases. All the proteins, except for the two loops, are colored in *light gray*. Loops of AlyP (PDB entry 1UAI), AlgAT5 (PDB entry 5ZQI), FlAlaA (PDB entry 5Y33), AlyA (PDB entry 4OZX), AlyQ (PDB entry 5XNR), PA1167 (PDB entry 1VAV), A1-II (PDB entry 2CWS), AlyA5 (PDB entry 4BE3), AlyA1 (PDB entry 3ZPY), AlyB (PDB entry 5ZU5), and AlyC3 are colored in *green, red, orange, light blue, purple, cyan, pink, wheat, yellow, deep teal, and blue*, respectively.

mutants, we suggest that residues Arg⁸² and Tyr¹⁹⁰ are essential for the positioning of the repeated units of alginate in AlyC3. This suggestion is supported by the biochemical data showing that AlyC3 cannot degrade a substrate smaller than trimannuronate (Fig. 3A). This is likely because sugar chains smaller than trimannuronate are too short to be positioned by the residues at the two ends of the catalytic cavity. Indeed, in the structure of H127A/Y244A–M2, Arg⁸² has no interaction with the bound M2, unable to help to position M2 accurately. This may explain why the distances between M2 and the catalytic residues His¹²⁷ and Tyr²⁴⁴ are rather far apart (4.74 and 4.12 Å, respectively) (Fig. 6E). In contrast, in the model of AlyC3 complexed with tetramannuronate (M4), the location of the M4 substrate

moves toward Arg⁸² compared with the location of M2 in the H127A/Y244A–M2 complex (Fig. 6G), and the distances between M4 and the catalytic residues His¹²⁷ and Tyr²⁴⁴ decrease to 4.20 and 3.45 Å, respectively (Fig. 6G). Taken together, these results demonstrate the roles of Arg⁸² and Tyr¹⁹⁰ in substrate positioning.

In the ulvan lyase LOR_107, Asn²⁶³ changes its conformation to pin the substrate to the active site (40). Similarly, in AlyC3, the side chain of Arg⁷⁸ in the complex structure apparently migrates downwards compared with that in the WT structure (Fig. 6E), suggesting that Arg⁷⁸ at the center of the catalytic center is also likely to assist with substrate positioning, in addition to being the neutralizer. Therefore, in AlyC3, the substrate can

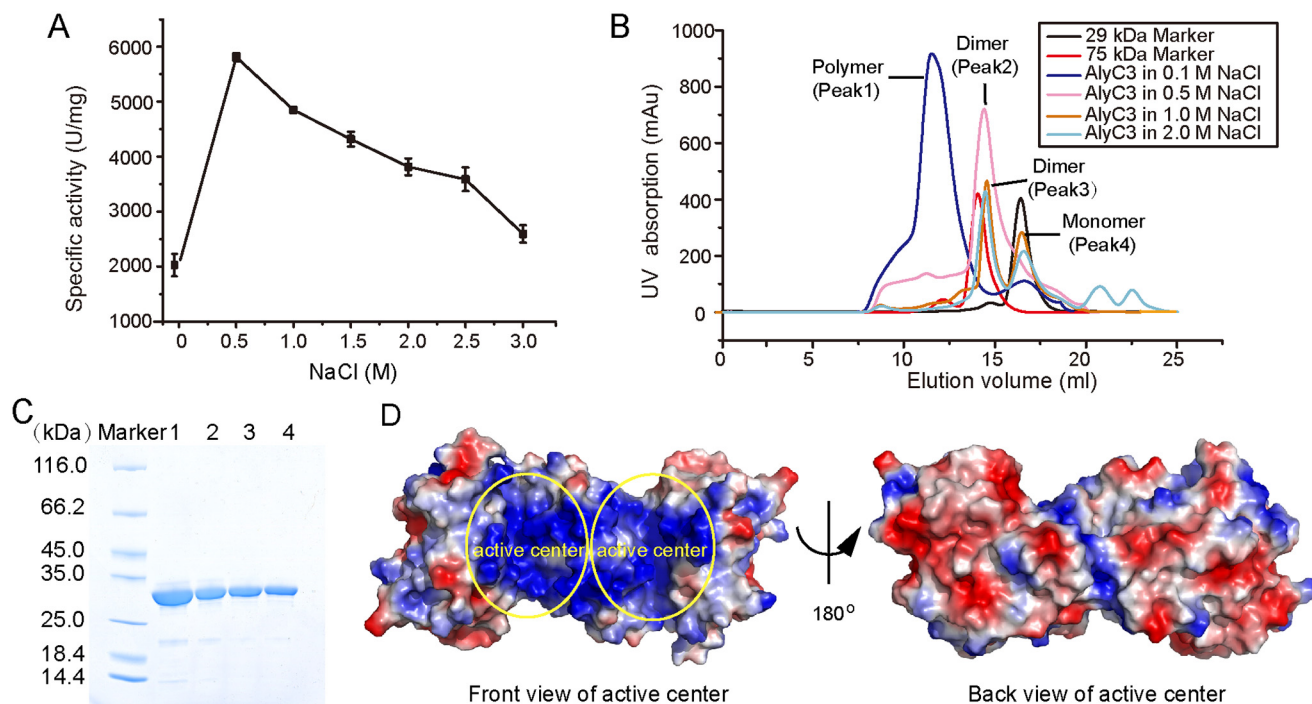


Figure 5. Analysis of the adaptation of AlyC3 to the seawater salinity. *A*, the effect of salinity on AlyC3 activity. *B*, aggregation states of AlyC3 in different NaCl concentrations. Conalbumin (75 kDa) and carbonic anhydrase (29 kDa) from GE Healthcare were used as protein size standards to analyze the polymeric form of proteins. *C*, SDS-PAGE analysis of AlyC3 at different aggregation states. Lanes 1–4 correspond to peaks 1–4 in *B*, respectively. *D*, electrostatic surface view of the WT AlyC3 dimer.

be accurately positioned by the amino acid residues at both ends (Arg⁸² and Tyr¹⁹⁰) and the center (Arg⁷⁸) of the catalytic center.

Analysis of residues involved in substrate positioning in other PL7 alginate lyases

Arg⁸² of AlyC3 is highly conserved in subfamily 6 alginate lyases (Fig. S3), suggesting a pivotal role of this residue in the catalysis of other subfamily 6 alginate lyases. To confirm this hypothesis, we performed enzymatic assays of another subfamily 6 alginate lyase AlxM (GenBankTM accession number CAA49630.1). When mutating Arg¹⁰¹ (corresponding to Arg⁸² of AlyC3) of AlxM to alanine, the specific activity and V_{max} of R101A toward its optimum substrate PM decreased ~78.87 and 77.91%, respectively, but its K_m remains comparable with that of the WT AlxM (Table 3). Thus, mutation of R101A resulted in changes in AlxM similar to those in AlyC3 caused by the mutation of R82A, suggesting that Arg¹⁰¹ is likely involved in substrate positioning in AlxM, akin to Arg⁸² in AlyC3.

Moreover, we found that Arg⁸² of AlyC3 is also highly conserved in PL7 alginate lyases of the other subfamilies (Fig. 6D), and similar mutational results have been reported on the amino acid residue Arg¹⁵⁰ (corresponding to Arg⁸² of AlyC3) in A1- II (17). The PL7 alginate lyases contain three consensus sequences, N-terminal RXEL(V)R, QI(V)H, and C-terminal YFKXG-XYXQ, and the key residues for catalysis (underlined) are all present in these sequences (41). The highly conserved Arg⁸² of AlyC3 is also in the important consensus RXEL(V)R, indicating the importance of this arginine in PL7 alginate lyases. There-

fore, residues corresponding to Arg⁸² of AlyC3 in other PL7 alginate lyases may have similar functions for substrate positioning.

The proposed catalytic process of AlyC3

Based on the above structural and biochemical results, the catalytic process of AlyC3 for alginate degradation was proposed (Fig. 7). When the substrate approaches the catalytic cavity, the positive charges of the groove and specific residues, such as Tyr⁴⁴, Lys¹²⁹, His¹⁴¹, Lys¹⁷¹, and Gln²⁴⁶, help the binding of the substrate. Different from other PL7 alginate lyases (17, 42), the substrate-binding process in AlyC3 does not need the opening of loop 1. In the process of binding, residues Arg⁸² and Tyr¹⁹⁰ at the two ends of the catalytic center help the positioning of the repeated units. Arg⁷⁸ at the center of the catalytic center is also involved in substrate positioning. As such, the substrate is aligned at the appropriate position, and the key residues His¹²⁷, Tyr²⁴⁴, Arg⁷⁸, and Gln¹²⁵ mediate the catalytic reaction. Arg⁷⁸ and Gln¹²⁵ neutralize the negative charge on the carboxylic group of +1 subsite, activating the C α hydrogen of M + 1. His¹²⁷ functions as the catalytic base to attack the C α of M + 1, leading to the formation of an unstable substrate-AlyC3 intermediate, in which both the C α -H bond and the C β -O bond between M + 1 and M - 1 are weakened. Along with the formation of the N-H bond of His¹²⁷ in AlyC3, the α -H of the substrate is released, and the C β -O bond between M + 1 and M - 1 is broken immediately. Tyr²⁴⁴ functions as a catalytic acid to accept electron and helps to cleave the C β -O bond, after which a trisaccharide product is released. With the help of Lys¹²⁹, His¹⁴¹, Lys¹⁷¹, Gln²⁴⁶, Arg⁸², and Tyr¹⁹⁰, a new

Substrate positioning of an alginate lyase

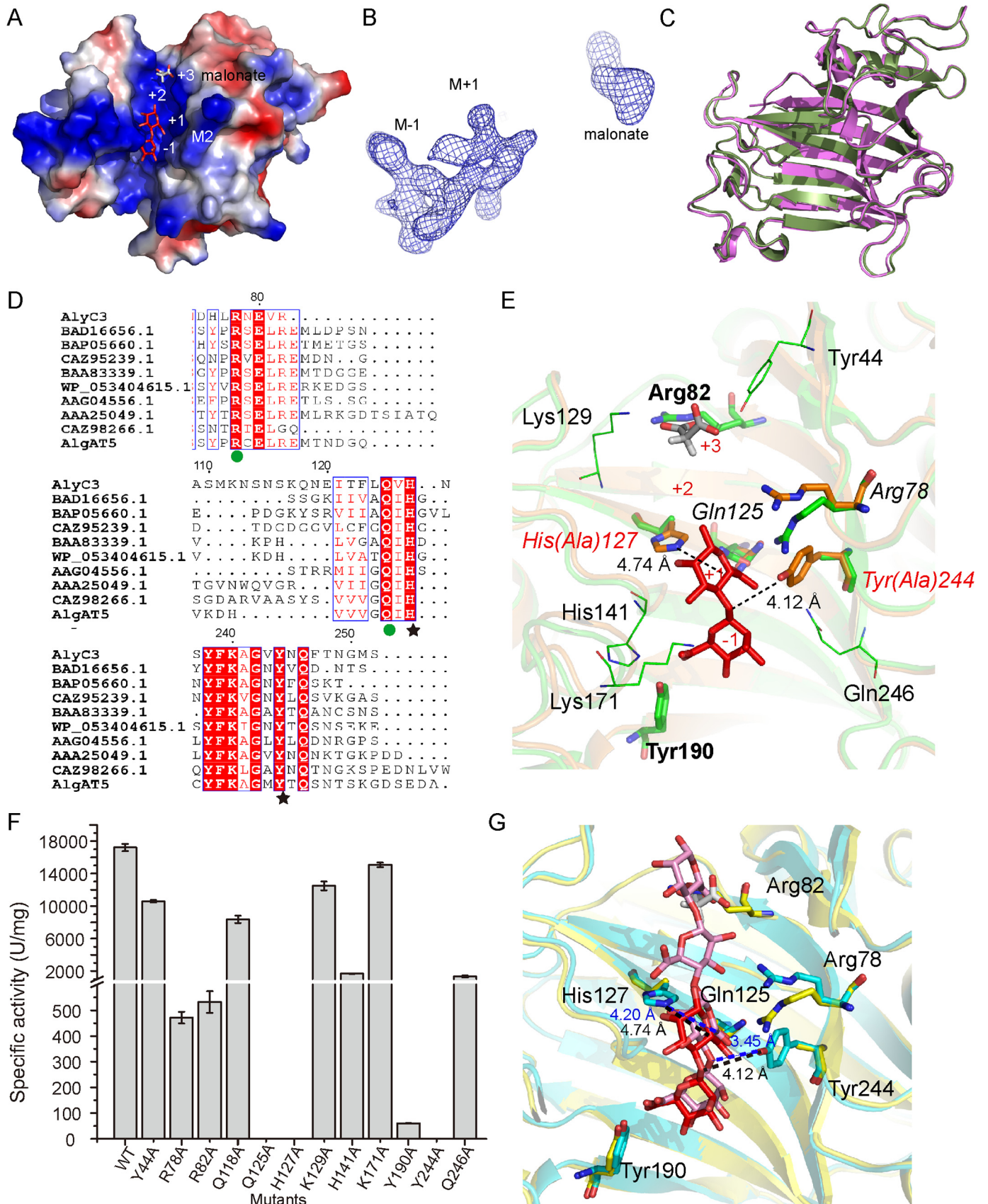


Table 2
Kinetic parameters of AlyC3 and the mutants

| Enzyme | K_m | V_{max} |
|--------|-----------------|---------------------|
| | mg/ml | units/mg |
| WT | 0.24 ± 0.05 | 19,704.73 ± 1865.49 |
| Y44A | 1.16 ± 0.30 | 12,072.99 ± 1722.07 |
| R78A | 0.26 ± 0.05 | 989.50 ± 94.92 |
| R82A | 0.30 ± 0.03 | 1763.44 ± 115.50 |
| H127A | ND ^a | ND |
| K129A | 0.43 ± 0.03 | 11,217.29 ± 364.08 |
| Q125A | ND | ND |
| H141A | 5.28 ± 1.11 | 6976.64 ± 852.13 |
| K171A | 1.17 ± 0.30 | 16,941.23 ± 2416.48 |
| Y190A | 0.28 ± 0.03 | 240.23 ± 8.82 |
| Y244A | ND | ND |
| Q246A | 0.85 ± 0.19 | 2224.48 ± 295.87 |

^aND, not detected.**Table 3**
Kinetic parameters of AlxM and its mutant

| Enzyme | Specific activity | K_m | V_{max} |
|--------|-------------------|-------------|-----------|
| | units/mg | mg/ml | units/mg |
| AlxM | 8410.58 ± 416.91 | 0.13 ± 0.01 | 8667.88 |
| R101A | 1776.92 ± 13.64 | 0.19 ± 0.02 | 1914.89 |

sugar chain will be bound and positioned at the right position again to initiate the next catalytic cycle.

Conclusion

Although a large number of alginate lyases have been reported, studies on alginate lyases from cold polar region are relatively rare. In this study, we characterized a novel cold-active and PM-specific endo-alginate lyase, AlyC3, from a bacterium isolated from the Arctic Ocean. This new enzyme belongs to subfamily 6 of the PL7 family, a new PM-specific subfamily proposed in this study based on phylogenetic analysis and enzymatic characterization. Structure analysis shows that AlyC3 is a dimeric enzyme that is the first reported dimeric endotype alginate lyase structure. Further analysis suggests that dimerization is a strategy of AlyC3 to adapt to the seawater salinity, which is different from the other salt-activated alginate lyases.

Although the mechanisms of many alginate lyases for substrate recognition and catalysis have been revealed, there is no report on how the substrate polymer is accurately positioned in the catalytic center for catalysis in alginate lyases. In this study, by combining the structural analysis with the kinetic parameters determination and multiple sequence alignment, three amino acid residues (Arg⁷⁸, Arg⁸², and Tyr¹⁹⁰) in AlyC3 were

found to be involved in the accurate positioning of the substrate polymer in the catalytic center, and the catalytic process of AlyC3 was proposed, including the recognition and positioning of the substrate and the electron transfer in the active center.

The results in this study provide new insight into alginate lyases and the mechanisms of alginate degradation. As a polar origin enzyme, some adaptive characters of AlyC3 to the Arctic Ocean environment have been revealed, such as cold-active and dimerization. Further investigation on its environmental adaptation mechanism will deepen our understanding of the relationship of polar enzymes and its extreme environment.

Experimental procedures

Materials and strains

Sodium alginate (viscosity, 15–20 cps) was purchased from Sigma (America). PM, PG (6–8 kDa), and oligosaccharide substrates were purchased from Zzstandard (China). Strain *Psychromonas* sp. C-3 was isolated from Arctic brown alga *Laminaria* and grown in marine broth 2216 (BD Biosciences–Difco) at 20 °C (20). *E. coli* was cultivated in LB medium at 37 °C.

Gene cloning and mutagenesis

The genome DNA of strain C-3 was shotgun-sequenced. Gene *alyC3* (GenBankTM accession number MT495249) in the genome was deduced to encode an alginate lyase. The *alyC3* gene was amplified from the genomic DNA of strain C-3 via PCR and cloned into the vector pET-22b between the restriction sites NdeI and XhoI along with a C-terminal His tag. Site-directed mutations on AlyC3 were conducted with the plasmid pET22b-*alyC3* as the template using a QuikChange kit (Agilent Technologies).

Sequence analysis

The residues encoding a putative signal peptide were predicted by the SignalP 4.1 server. Sequence alignment was performed by ClustalX, and alignment figures were processed using ESPrpt 3.0 server (43). The phylogenetic trees were constructed based on related alginate lyase sequences of the PL7 family using MEGA 7.0.

Protein expression and purification

Recombinant proteins of WT AlyC3 and its mutants were overexpressed in *E. coli* BL21 (DE3), which was grown at 15 °C at 100 rpm for 16 h in LB broth containing 100 μg/ml

Figure 6. Analysis of the important amino acid residues in the active center of AlyC3. A, electrostatic surface view of H127A/Y244A–M2 monomer. The bound M2 and malonate molecules are shown as red and gray sticks, respectively. B, $F_o - F_c$ omit map of the M2 and malonate molecules in the H127A/Y244A–M2 complex. The simulated annealing $F_o - F_c$ omit map was generated using the Phenix program by omitting the M2 and malonate molecules. The resulting electron density map was contoured at 3σ . C, structural superposition alignment of WT AlyC3 and H127A/Y244A–M2. WT AlyC3 and H127A/Y244A–M2 are presented in green and purple, respectively. D, sequence alignment of PL7 alginate lyases. Black stars indicate the catalytic acid/base. Green circles indicate the neutralization residues. The figure was prepared using ESPrpt program. E, the residues interacting with M2 in H127A/Y244A–M2. WT AlyC3 and H127A/Y244A–M2 are in orange and green, respectively. M2 and malonate are shown as red and gray sticks, respectively. Side chains of His¹²⁷, Tyr²⁴⁴, Arg⁷⁸, and Gln¹²⁵ in WT AlyC3 are depicted as orange sticks. Tyr¹⁹⁰ and Arg⁸² in H127A/Y244A–M2 are shown as green sticks. Other residues are depicted as green lines. The hydrogen bonds are represented by dotted lines. F, the enzymatic activities of AlyC3 mutants. Experiments were conducted at 20 °C for 5 min in a 200-μl mixture containing enzymes at different concentrations and 2 mg/ml PM in 50 mM Tris-HCl (pH 8.0) containing 0.5 M NaCl. G, structural comparison of H127A/Y244A–M2 complex with the simulated model of the AlyC3–M4 complex. The AlyC3–M4 and H127A/Y244A–M2 are shown in cyan and yellow, respectively. The M2 (dimannuronate), malonate, and simulated M4 (tetramannuronate) are shown as red, gray, and pink sticks, respectively. The distances between the catalytic residues (His¹²⁷ and Tyr⁴⁴) to M2 and M4 are shown as black and blue dotted lines, respectively.

Substrate positioning of an alginate lyase

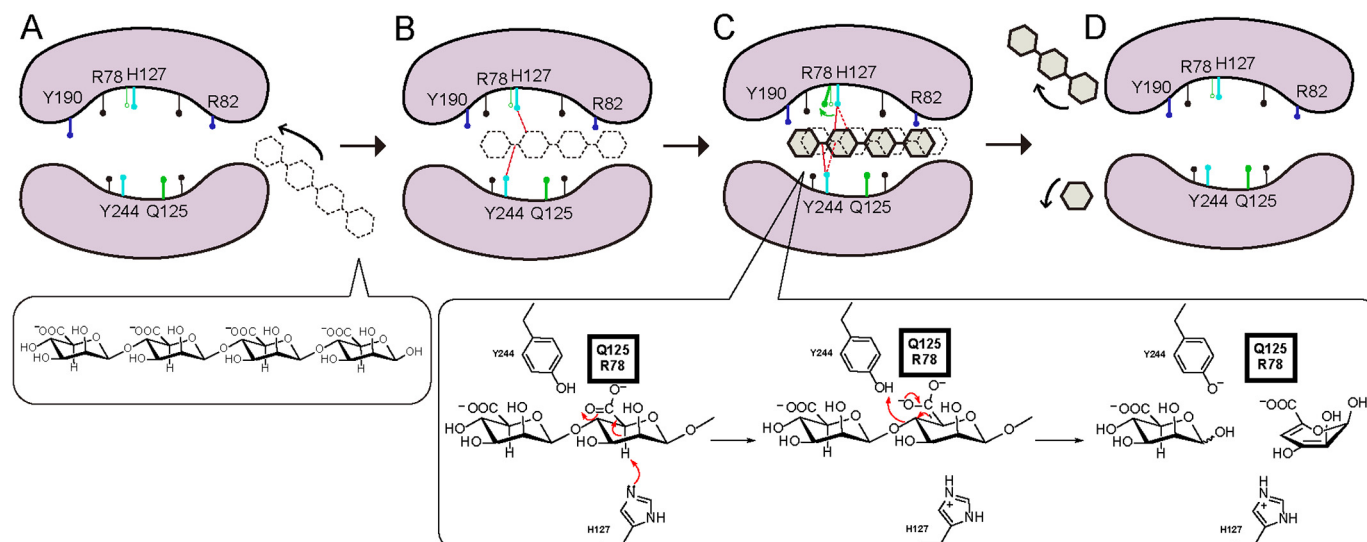


Figure 7. Schematic diagram of the proposed catalytic process of AlyC3. *A*, the substrate (take the tetramannuronate as an example) approaches the catalytic cavity. *B*, when the substrate enters the catalytic cavity, the positive charges of the groove and specific residues (black sticks) like Tyr⁴⁴, Lys¹²⁹, His¹⁴¹, Lys¹⁷¹, and Gln²⁴⁶ help the binding of the substrate. At this time, the tetramer is shown as a black dotted line, and the distances between the catalytic residues and substrate, which are shown as red dotted lines, are slightly far, affecting the catalytic efficiency. *C*, in the process of binding, residues Arg⁸² and Tyr¹⁹⁰ help the accurate positioning of the substrate, and thus the catalytic residues are close to the substrate, ensuring the high catalytic efficiency. Meanwhile, the side chain of Arg⁷⁸ migrates to assist with substrate positioning. At this time, the tetramer is shown as a black solid line, and the distances between the catalytic residues to the substrate are shown as red solid lines. The key residues His¹²⁷, Tyr²⁴⁴, Arg⁷⁸, and Gln¹²⁵ mediate the catalytic reaction. Arg⁷⁸ and Gln¹²⁵ form interactions with the carboxyl group of the M + 1 and activate the C α hydrogen of M + 1. His¹²⁷ functions as the catalytic base to attack the C α of M + 1, and Tyr²⁴⁴ functions as the catalytic acid to accept an electron. Electron transfer is presented with red arrows. *D*, the products are released after the degradation reaction.

ampicillin under the induction of 0.3 mM isopropyl β -D-1-thiogalactopyranoside. Selenomethionine (SeMet)-labeled AlyC3 was expressed by inhibiting endogenous methionine biosynthesis in *E. coli* BL21 (DE3). The cells grown overnight in LB medium were harvested and inoculated in the M9 medium containing 100 mg/liter of lysine, phenylalanine and threonine, 50 mg/liter of isoleucine, leucine, and valine, 5.2% (w/v) glucose, and 0.65% (w/v) yeast nitrogen base, which were then grown at 37 °C. When the A_{600} reached 0.6, the culture was cooled to 15 °C, and 50 mg/liter L-SeMet was added. 15 min later, the culture was incubated at 15 °C at 100 rpm for 14 h under the induction of 0.4 mM isopropyl β -D-1-thiogalactopyranoside.

The recombinant proteins were first purified by nickel-nitrilotriacetic acid resin (Qiagen) and then fractionated by gel filtration on a Superdex G-200 column (GE Healthcare). Conalbumin (75 kDa) and carbonic anhydrase (29 kDa) from GE Healthcare were used as protein size standards to analyze the polymeric form of proteins.

Biochemical characterization of AlyC3

Protein concentration was determined with BSA as the standard using a BCA protein assay kit (Thermo). The activities of WT AlyC3 and its mutants toward substrates were measured by the UV absorption spectrometry method (31). Briefly, a 200- μ l mixture containing 0.6 μ g/ml enzyme and 2 mg/ml substrate in 50 mM Tris-HCl (pH 8.0) was incubated at 20 °C for 5 min. The reaction was terminated by heat inactivation by boiling for 10 min. Then an increase in the absorbance at 235 nm (A_{235}) resulted from the release of unsaturated uronic in the mixture was monitored. One unit of enzyme activity was defined as the amount of enzyme required to produce an increase of 0.1/min

at 235 nm. The action mode and degrading products of AlyC3 were analyzed by using PM oligosaccharides as the substrates. The degradation reaction was carried out in 0.5 M NaCl at pH 8.0 and 20 °C for 10 min. The concentrations of the enzyme and substrate used were 7 μ g/ml and 2 mg/ml, respectively. The resultant degradation products were analyzed by HPLC on a Superdex Peptide 10/300 GL column (GE Healthcare) at a flow rate of 0.35 ml/min using 0.2 M ammonium hydrogen carbonate as the running buffer. Elution was monitored at 210 nm using a UV detector. LabSolutions software was used for online monitoring and data analysis (44). The kinetic parameters of the purified enzymes were determined by measuring the enzyme activities toward the substrate PM at different concentrations (0.05–6 mg/ml) in 0.5 M NaCl and analyzed by the Michaelis–Menten equation using Origin 8.5 software.

Crystallization and data collection

WT AlyC3 (10 mg/ml) was crystallized at 18 °C by the sitting-drop method in the buffer containing 20% (w/v) PEG 3350 and 0.2 M succinic acid (pH 7.0). Crystals of SeMet-AlyC3 (6 mg/ml) were grown in the buffer containing 0.1 M Bis-Tris (pH 6.5) and 25% (w/v) PEG 3350. The inactive mutant H127A/Y244A (6 mg/ml) mixed with M2 at a molar ratio of 1:10 was crystallized at 18 °C by the hanging-drop method in the buffer containing 0.1 M Bis-Tris propane (pH 7.5), 0.2 M sodium malonate, and 19% (w/v) PEG 3350. X-ray diffraction data were collected on the BL17U1 Beamline at the Synchrotron Radiation Facility using detector ADSC Quantum 315r (45). The initial diffraction data sets were processed by HKL2000. The data collection statistics are shown in Table 1.

Structure determination and refinement

Heavy atoms were solved by the single-wavelength anomalous diffraction method using the Phenix program Autosol (46). Initial model building was finished by the Phenix program AutoBuild (46). Refinement of the AlyC3 structure was performed by the Phenix program Refine (46) and Coot (47) alternately. The quality of the final model is summarized in Table 1. All the structure figures were processed using the program PyMOL.

Model docking

The refined model of AlyC3 was used for docking using a genetic algorithm called simple evolution by Molegro Virtual Docker v6.0. The default docking parameters were adopted except that the number of runs, the max iterations, and the population size in each run were set to 50, 3000, and 100, respectively. Cluster analysis was performed on different poses with a RMSD threshold of 1.0 Å. For each ligand, 50 poses were returned and ranked with regard to their MolDock score energy. The best reasonable binding mode with relative lower binding energy was selected from the above poses according to the location of M2 in the H127A/Y244A–M2 complex. The representation of the protein structure was generated by PyMOL.

Data availability

The atomic coordinates and structure factors of AlyC3 (codes 7C8G and 7C8F) have been deposited in the Protein Data Bank.

Acknowledgments—We thank the staffs from BL18U1 and BL19U1 Beamlines of the National Facility for Protein Sciences Shanghai and the Shanghai Synchrotron Radiation Facility for assistance during data collection. We also thank Xiaojun Li and Haiyan Sui from the State Key Laboratory of Microbial Technology of Shandong University for help and guidance with the single crystal X-ray diffractometer.

Author contributions—F. X. formal analysis; F. X., X.-L. C., and C.-Y. L. validation; F. X., X.-H. S., F. D., and P. W. investigation; F. X. writing-original draft; X.-L. C., Y.-Z. Z., and P. W. methodology; X.-L. C., P.-Y. L., Y.-Z. Z., and P. W. project administration; X.-L. C., Y. C., and Y.-Z. Z. writing-review and editing; C.-Y. L., HD, and P. W. software; Y.-Z. Z. conceptualization.

Funding and additional information—This work was supported by Grant 2018YFC1406700 from the National Key Research and Development Program of China; Grants 91851205, 31870052, 31800107, U1706207, 91751101, 41706152, and 41676180 from the National Science Foundation of China; Grant 2019JZZY010817 from the Major Scientific and Technological Innovation Project of Shandong Province; Grant tspd20181203 from the Program of Shandong for Taishan Scholars; Grants 2017ASTCP-OS14 and QNLM2016ORP0310 from the AoShan Talents Cultivation Program Supported by Qingdao National Laboratory for Marine Science and Technology; and Grant 2017WJH57 from the Young Scholars Program of Shandong University.

Conflict of interest—The authors declare that they have no conflicts of interest with the contents of this article.

Abbreviations—The abbreviations used are: PDB, Protein Data Bank; RMSD, root-mean-square deviation; PM, polymannuronate; PG, polyguluronate; PL, polysaccharide lyase; M, mannuronate; Δ, 4-deoxy-1-erythro-hex-4-enopyranosyluronic acid; SA, sheet A; SB, sheet B; SeMet, selenomethionine.

References

- Meillisa, A., Woo, H. C., and Chun, B. S. (2015) Production of monosaccharides and bio-active compounds derived from marine polysaccharides using subcritical water hydrolysis. *Food Chem.* **171**, 70–77 [CrossRef](#) [Medline](#)
- Smith, S. V. (1981) Marine macrophytes as a global carbon sink. *Science* **211**, 838–840 [CrossRef](#) [Medline](#)
- Usov, A. I., Bilan, M. I., and Klochkova, N. G. (1995) Polysaccharides of algae: 48. Polysaccharide composition of several calcareous red algae: isolation of alginate from *Corallina pilulifera* P. et R. (Rhodophyta, Corallinales). *Bot. Mar.* **38**, 43–51 [CrossRef](#)
- Gorin, P. A. J., and Spencer, J. F. T. (1966) Exocellular alginic acid from *Azotobacter vinelandii*. *Can. J. Chem.* **44**, 993–998 [CrossRef](#)
- Linker, A., and Jones, R. S. (1966) A new polysaccharide resembling alginic acid isolated from *Pseudomonads*. *J. Biol. Chem.* **241**, 3845–3851 [Medline](#)
- Hu, X. K., Jiang, X. L., Hwang, H. M., Liu, S. L., and Guan, H. S. (2004) Promotive effects of alginate-derived oligosaccharide on maize seed germination. *J. Appl. Phycol.* **16**, 73–76 [CrossRef](#)
- Iwamoto, M., Kurachi, M., Nakashima, T., Kim, D., Yamaguchi, K., Oda, T., Iwamoto, Y., and Muramatsu, T. (2005) Structure–activity relationship of alginate oligosaccharides in the induction of cytokine production from RAW264.7 cells. *FEBS Lett.* **579**, 4423–4429 [CrossRef](#) [Medline](#)
- Wong, T. Y., Preston, L. A., and Schiller, N. L. (2000) Alginate lyase: review of major sources and enzyme characteristics, structure–function analysis, biological roles, and applications. *Annu. Rev. Microbiol.* **54**, 289–340 [CrossRef](#) [Medline](#)
- Islan, G. A., Bosio, V. E., and Castro, G. R. (2013) Alginate lyase and ciprofloxacin co-immobilization on biopolymeric microspheres for cystic fibrosis treatment. *Macromol. Biosci.* **13**, 1238–1248 [CrossRef](#) [Medline](#)
- Wargacki, A. J., Leonard, E., Win, M. N., Regitsky, D. D., Santos, C. N., Kim, P. B., Cooper, S. R., Raisner, R. M., Herman, A., Sivitz, A. B., Lakshmanaswamy, A., Kashiyama, Y., Baker, D., and Yoshikuni, Y. (2012) An engineered microbial platform for direct biofuel production from brown macroalgae. *Science* **335**, 308–313 [CrossRef](#) [Medline](#)
- Enquist-Newman, M., Faust, A. M., Bravo, D. D., Santos, C. N., Raisner, R. M., Hanel, A., Sarvabhowman, P., Le, C., Regitsky, D. D., Cooper, S. R., Peereboom, L., Clark, A., Martinez, Y., Goldsmith, J., Cho, M. Y., et al. (2014) Efficient ethanol production from brown macroalgae sugars by a synthetic yeast platform. *Nature* **505**, 239–243 [CrossRef](#) [Medline](#)
- Helbert, W., Poulet, L., Drouillard, S., Mathieu, S., Loiodice, M., Couturier, M., Lombard, V., Terrapon, N., Turchetto, J., Vincentelli, R., and Henrisat, B. (2019) Discovery of novel carbohydrate-active enzymes through the rational exploration of the protein sequences space. *Proc. Natl. Acad. Sci. U.S.A.* **116**, 6063–6068 [CrossRef](#) [Medline](#)
- Hehemann, J. H., Boraston, A. B., and Czjzek, M. (2014) A sweet new wave: structures and mechanisms of enzymes that digest polysaccharides from marine algae. *Curr. Opin. Struct. Biol.* **28**, 77–86 [CrossRef](#) [Medline](#)
- Thomas, F., Lundqvist, L. C. E., Jam, M., Jeudy, A., Barbeyron, T., Sandström, C., Michel, G., and Czjzek, M. (2013) Comparative characterization of two marine alginate lyases from *Zobellia galactanivorans* reveals distinct modes of action and exquisite adaptation to their natural substrate. *J. Biol. Chem.* **288**, 23021–23037 [CrossRef](#) [Medline](#)
- Osawa, T., Matsubara, Y., Muramatsu, T., Kimura, M., and Kakuta, Y. (2005) Crystal structure of the alginate (poly α-l-guluronate) lyase from *Corynebacterium* sp. at 1.2 Å resolution. *J. Mol. Biol.* **345**, 1111–1118 [CrossRef](#) [Medline](#)

Substrate positioning of an alginate lyase

16. Qin, H. M., Miyakawa, T., Inoue, A., Nishiyama, R., Nakamura, A., Asano, A., Ojima, T., and Tanokura, M. (2018) Structural basis for controlling the enzymatic properties of polymannuronate preferred alginate lyase FIAlyA from the PL-7 family. *Chem. Commun. (Camb.)* **54**, 555–558 [CrossRef Medline](#)
17. Yamasaki, M., Ogura, K., Hashimoto, W., Mikami, B., and Murata, K. (2005) A structural basis for depolymerization of alginate by polysaccharide lyase family-7. *J. Mol. Biol.* **352**, 11–21 [CrossRef Medline](#)
18. Lombard, V., Bernard, T., Rancurel, C., Brumer, H., Coutinho, P. M., and Henrissat, B. (2010) A hierarchical classification of polysaccharide lyases for glycogenomics. *Biochem. J.* **432**, 437–444 [CrossRef Medline](#)
19. Vuoristo, K. S., Fredriksen, L., Oftebro, M., Arntzen, M. O., Aarstad, O. A., Stokke, R., Steen, I. H., Hansen, L. D., Schüller, R. B., Aachmann, F. L., Horn, S. J., and Eijsink, V. G. H. (2019) Production, characterization, and application of an alginate lyase, AMOR_PL7A, from hot vents in the Arctic mid-ocean ridge. *J. Agric. Food Chem.* **67**, 2936–2945 [CrossRef Medline](#)
20. Dong, S., Yang, J., Zhang, X. Y., Shi, M., Song, X. Y., Chen, X. L., and Zhang, Y. Z. (2012) Cultivable alginate lyase-excreting bacteria associated with the Arctic brown alga *Laminaria*. *Mar. Drugs* **10**, 2481–2491 [CrossRef Medline](#)
21. Kawamoto, H., Horibe, A., Miki, Y., Kimura, T., Tanaka, K., Nakagawa, T., Kawamukai, M., and Matsuda, H. (2006) Cloning and sequencing analysis of alginate lyase genes from the marine bacterium *Vibrio* sp. O₂. *Mar. Biotechnol. (NY)* **8**, 481–490 [CrossRef Medline](#)
22. Malissard, M., Duez, C., Guinand, M., Vacheron, M. J., Michel, G., Marty, N., Joris, B., Thamm, L., and Ghuysen, J. M. (1993) Sequence of a gene encoding a (poly ManA) alginate lyase active on *Pseudomonas aeruginosa* alginate. *FEMS Microbiol. Lett.* **110**, 101–106 [CrossRef Medline](#)
23. Uchimura, K., Miyazaki, M., Nogi, Y., Kobayashi, T., and Horikoshi, K. (2010) Cloning and sequencing of alginate lyase genes from deep-sea strains of *Vibrio* and *Agarivorans* and characterization of a new *Vibrio* enzyme. *Mar. Biotechnol. (NY)* **12**, 526–533 [CrossRef Medline](#)
24. Li, S., Yang, X., Zhang, L., Yu, W., and Han, F. (2015) Cloning, expression, and characterization of a cold-adapted and surfactant-stable alginate lyase from marine bacterium *Agarivorans* sp. L11. *J. Microbiol. Biotechnol.* **25**, 681–686 [CrossRef Medline](#)
25. Gao, S., Z. Z., Li, S., Su, H., Tang, L., Tan, Y., Yu, W., and Han, F. (2018) Characterization of a new endo-type polysaccharide lyase (PL) family 6 alginate lyase with cold-adapted and metal ions-resisted property. *Int. J. Biol. Macromol.* **120**, 729–735 [CrossRef Medline](#)
26. Inoue, A., Mashino, C., Uji, T., Saga, N., Mikami, K., and Ojima, T. (2015) Characterization of an eukaryotic PL-7 alginate lyase in the marine red alga *Pyropia yezoensis*. *Curr. Biotechnol.* **4**, 240–248 [CrossRef Medline](#)
27. Chen, X. L., Dong, S., Xu, F., Dong, F., Li, P. Y., Zhang, X. Y., Zhou, B. C., Zhang, Y. Z., and Xie, B. B. (2016) Characterization of a new cold-adapted and salt-activated polysaccharide lyase family 7 alginate lyase from *Pseudoalteromonas* sp. SM0524. *Front. Microbiol.* **7**, 1120 [CrossRef Medline](#)
28. Wang, Z. P., Cao, M., Li, B., Ji, X. F., Zhang, X. Y., Zhang, Y. Q., and Wang, H. Y. (2020) Cloning, secretory expression and characterization of a unique pH-stable and cold-adapted alginate lyase. *Mar. Drugs* **18**, 189 [CrossRef](#)
29. Yamasaki, M., Moriawaki, S., Miyake, O., Hashimoto, W., Murata, K., and Mikami, B. (2004) Structure and function of a hypothetical *Pseudomonas aeruginosa* protein PA1167 classified into family PL-7: a novel alginate lyase with a beta-sandwich fold. *J. Biol. Chem.* **279**, 31863–31872 [CrossRef Medline](#)
30. Ogura, K., Yamasaki, M., Yamada, T., Mikami, B., Hashimoto, W., and Murata, K. (2009) Crystal structure of family 14 polysaccharide lyase with pH-dependent modes of action. *J. Biol. Chem.* **284**, 35572–35579 [CrossRef Medline](#)
31. Dong, S., Wei, T. D., Chen, X. L., Li, C. Y., Wang, P., Xie, B. B., Qin, Q. L., Zhang, X. Y., Pang, X. H., Zhou, B. C., and Zhang, Y. Z. (2014) Molecular insight into the role of the N-terminal extension in the maturation, substrate recognition, and catalysis of a bacterial alginate lyase from polysaccharide lyase family 18. *J. Biol. Chem.* **289**, 29558–29569 [CrossRef Medline](#)
32. Dong, F., Xu, F., Chen, X. L., Li, P. Y., Li, C. Y., Li, F. C., Chen, Y., Wang, P., and Zhang, Y. Z. (2019) Alginate lyase Aly36B is a new bacterial member of the polysaccharide lyase family 36 and catalyzes by a novel mechanism with lysine as both the catalytic base and catalytic acid. *J. Mol. Biol.* **431**, 4897–4909 [CrossRef Medline](#)
33. Xu, F., Dong, F., Wang, P., Cao, H. Y., Li, C. Y., Li, P. Y., Pang, X. H., Zhang, Y. Z., and Chen, X. L. (2017) Novel molecular insights into the catalytic mechanism of marine bacterial alginate lyase AlyGC from polysaccharide lyase family 6. *J. Biol. Chem.* **292**, 4457–4468 [CrossRef Medline](#)
34. Holm, L., and Rosenstrom, P. (2010) Dali server: conservation mapping in 3D. *Nucleic Acids Res.* **38**, W545–W549 [CrossRef Medline](#)
35. Ogura, K., Yamasaki, M., Mikami, B., Hashimoto, W., and Murata, K. (2008) Substrate recognition by family 7 alginate lyase from *Sphingomonas* sp. A1. *J. Mol. Biol.* **380**, 373–385 [CrossRef Medline](#)
36. Zeng, Y. X., Qiao, Z. Y., Yu, Y., Li, H. R., and Luo, W. (2016) Diversity of bacterial dimethylsulfoniopropionate degradation genes in surface seawater of Arctic Kongsfjorden. *Sci. Rep.* **6**, 33031 [CrossRef Medline](#)
37. Hough, D. W., and Danson, M. J. (1999) Extremozymes. *Curr. Opin. Chem. Biol.* **3**, 39–46 [CrossRef Medline](#)
38. Huang, G. Y., Wang, Q. Z., Lu, M. Q., Xu, C., Li, F., Zhang, R. C., Liao, W., and Huang, S. S. (2018) AlgM4: a new salt-activated alginate lyase of the PL7 family with endolytic activity. *Mar. Drugs* **16**, 120 [CrossRef](#)
39. Xu, F., Wang, P., Zhang, Y. Z., and Chen, X. L. (2017) Alginate lyases: diversity of three dimensional structures and catalytic mechanisms. *Appl. Environ. Microbiol.* **84**, e02040-17 [CrossRef Medline](#)
40. Ulaganathan, T., Helbert, W., Kopel, M., Banin, E., and Cygler, M. (2018) Structure–function analyses of a PL24 family ulvan lyase reveal key features and suggest its catalytic mechanism. *J. Biol. Chem.* **293**, 4026–4036 [CrossRef Medline](#)
41. Sakatoku, A., Tanaka, D., and Nakamura, S. (2013) Purification and characterization of an alkaliphilic alginate lyase AlgMytC from *Saccharophagus* sp. Myt-1. *J. Mol. Biol.* **23**, 872–877 [CrossRef Medline](#)
42. Sim, P. F., Furusawa, G., and Teh, A. H. (2017) Functional and structural studies of a multidomain alginate lyase from *Persicobacter* sp. CCB-QB2. *Sci. Rep.* **7**, 13656 [CrossRef Medline](#)
43. Robert, X., and Gouet, P. (2014) Deciphering key features in protein structures with the new ENDscript server. *Nucleic Acids Res.* **42**, W320–W324 [CrossRef Medline](#)
44. Wang, Y. J., Jiang, W. X., Zhang, Y. S., Cao, H. Y., Zhang, Y., Chen, X. L., Li, C. Y., Wang, P., Zhang, Y. Z., Song, X. Y., and Li, P. Y. (2019) Structural insight into chitin degradation and thermostability of a novel endochitinase from the glycoside hydrolase family 18. *Front. Microbiol.* **10**, 2457 [CrossRef Medline](#)
45. Wang, Z. J., Pan, Q. Y., Yang, L. F., Zhou, H., Xu, C. Y., Yu, F., Wang, Q. S., Huang, S., and He, J. H. (2016) Automatic crystal centring procedure at the SSRF macromolecular crystallography beamline. *J. Synchrotron Radiat.* **23**, 1323–1332 [CrossRef Medline](#)
46. Adams, P. D., Grosse-Kunstleve, R. W., Hung, L. W., Ioerger, T. R., McCoy, A. J., Moriarty, N. W., Read, R. J., Sacchettini, J. C., Sauter, N. K., and Terwilliger, T. C. (2002) PHENIX: building new software for automated crystallographic structure determination. *Acta Crystallogr. D Biol. Crystallogr.* **58**, 1948–1954 [CrossRef Medline](#)
47. Emsley, P., and Cowtan, K. (2004) Coot: model-building tools for molecular graphics. *Acta Crystallogr. D Biol. Crystallogr.* **60**, 2126–2132 [CrossRef Medline](#)